REVISITING AN HISTORIC CASE STUDY: MONITORING AND ASSESSMENT OF ASR IN A DECOMMISSIONED LOCK STRUCTURE

Eric R. Giannini[1]*, Stephanie G. Wood[1], James H. Sanders[2], E. Rae Reed-Gore[3], Kyle L. Klaus[3], and Robert D. Moser[3]

[1] The University of Alabama, Tuscaloosa, AL, UNITED STATES OF AMERICA,

[2] U.S. Army Corps of Engineers, Mobile, AL, UNITED STATES OF AMERICA

[3] U.S. Army Engineer Research and Development Center, Vicksburg, MS, UNITED STATES OF AMERICA

Abstract

The Old Oliver Lock is a decommissioned lock structure on the Black Warrior River in Tuscaloosa, Alabama, USA. Constructed between 1937 and 1939, it was one of the first concrete structures in the eastern United States where ASR was identified as a cause of distress. A new lock went into service in 1992, but the old lock was not demolished and remains accessible for study.

In 2015, a team of researchers began a new study of the old lock structure. The detailed records available from the construction of the lock and the subsequent investigation of ASR that followed make it an ideal field structure for applying modern monitoring and assessment protocols.

The team selected four monoliths from the south wall of the lock with distinct variations in the degree of cracking for study. Core samples were also taken from each monolith under study and DEMEC targets for expansion monitoring were installed. This paper presents an overview of the study and selected results from petrography of the cores.

Keywords: hydraulic structure, case study, mechanical properties, petrography, structural monitoring

1 INTRODUCTION

The Old William Bacon Oliver Lock and Dam (Fig. 1) were constructed on the Black Warrior River in Tuscaloosa, Alabama, USA between 1937 and 1939 under the supervision of the Mobile District of the U.S. Army Corps of Engineers (USACE). By 1947, substantial cracking was noticed in some monoliths of the lock walls, prompting an investigation by Bryant Mather and others from the Waterways Experiment Station [1]. The investigation was primarily petrographic in nature, and would confirm the first known case of alkali-silica reaction (ASR) outside of the western United States.

Later investigation would determine the concrete to be "of generally good quality" despite the extensive cracking in some monoliths [2]. However, there were still efforts to monitor the progress of ASR in the structure. In 1974, the Mobile District of the U.S. Army Corps of Engineers installed leaded tacks on each side of the monolith joints and on each side of three significant cracks. Thirty-six inserts were set at the monolith joints on the land wall of the lock, twenty-three on the lower land wing wall, seventeen on the upper river wing wall, thirty-two on the river wall, and eleven on the lower river wing wall. In addition, seven monitoring points were set of the lock wall (three on the land wall and four on the river wall), plus four control pillars on land alongside the lock (Fig. 1). Alignment along each lock wall is done by sighting on a line between the monitoring points and measuring left or right movement of each alignment insert. Elevations of each alignment insert are also measured. Distances between the control pillars and each monitoring point on the lock walls were also taken to ensure that the monolith in which the monitoring points were installed had not moved.

The last measurements of alignment, elevations, and distances were made in 1986. The results of the measurements were plotted on rather crude graphs in the Mobile District, which did not appear to indicate any significant trends. The maximum alignment difference measured between the initial and last survey was 6.5 mm at monolith 63R/64R on the right lock wall and 4 mm at monolith joint 10L/11L on the left lock wall. However, experience at another lock undergoing alkali-carbonate reaction shows that it is better to plot graphs of individual inserts versus time. The maximum

* Correspondence to: ergiannini@eng.ua.edu

elevation difference measured for the right lock wall inserts was 13.3 mm between the initial and last survey was at R57, and the maximum elevation difference measured for the left lock wall was 8mm at monolith insert L12B. The graph of the elevation of insert 57R versus time appears to show a trend of increasing elevation. However, most of the apparent trend for 57R is a result of the initial and last readings. [3]

The lock was replaced by a new, larger, lock and dam structure located just downstream and was decommissioned in 1992. However, the old lock was not demolished and remains available for study. This paper presents the results of a recently-begun collaboration between researchers from The University of Alabama (UA) and the U.S. Army Engineer Research and Development Center (ERDC) to revisit Mather's historic investigation. The authors are applying modern assessment techniques for ASR-affected structures to determine the effects of ASR on the structure and understand why expansion has ceased.

2 MATERIALS AND METHODS

2.1 General

Several site visits were made by the authors between December 2012 and June 2015 for the purpose of conducting visual damage surveys of the structure, identifying sites of prior investigations, and logistical planning for core extraction and instrumentation. Core extraction took place in November 2015 and DEMEC targets were also installed for expansion monitoring at that time. Experimental testing of the cores began in January 2015 and includes a suite of mechanical, chemical, petrographic, and residual expansion tests.

2.2 Materials and mix designs

According to Mather [1] the concrete in the lock contained natural sand and gravel aggregates, water from the city of Tuscaloosa municipal water supply, and cement from two different mills. He notes a requirement for <8% C_3A in the cement, which suggests that these cements would have met the requirements for ASTM C150 Type II cement. Mather was unable to determine the alkali content of the cement, but noted that one of the cements came from an area where cements were "typically of rather high alkali content" during the time the lock was constructed. In his investigation, Mather found that monoliths constructed with this cement were noted to exhibit a substantially greater degree of distress than those containing cement from the other mill. Petrographic examination (conducted principally by Katherine Mather) of over 5,000 coarse aggregate particles in cores extracted in 1947 also determined that the gravel contained between 19 and 30 percent chalcedonic chert, which is known to be susceptible to ASR.

2.3 Methods for assessment and analysis

General

The methodology in this investigation was strongly influenced by research conducted over the past decade or so to develop improved protocols and techniques for assessing ASR-affected structures [4-7]. The investigation incorporates visual inspection, core extraction and testing, and in-situ monitoring to determine the current state of the structure and the impacts of ASR over the past 75-plus years since its construction.

Visual Survey and Monolith Selection

A visual survey of the land-side lock wall in May 2015 was conducted to determine the relative intensity of damage for each monolith. Damage ratings were given on a scale from 1 (least severe) to 5 (most severe). Figure 2 is presents a schematic of the structure with the damage ratings for each monolith. Based on this survey, monoliths 3, 20, 21, and 30 were selected for further investigation. Monoliths 3 and 30 were of interest because these contain stairs that descend to a platform at the level of the river. This allows for extracting cores both vertically and horizontally. Monoliths 20 and 21 were of interest because of the substantial difference in distress observed in these adjacent sections; monolith 20 contained the most severe distress of the thirty monoliths surveyed, while monolith 21 was assigned a damage rating of 2. Figure 3 illustrates the sharp contrast in damage between monoliths 20 and 21. Monoliths 3 and 20 were also cored as part of Mather's investigation.

The visual surveys found substantial evidence to indicate that expansion from ASR has ceased or slowed to a negligible rate. There were several concrete overlays placed after decommissioning of the lock that crossed major cracks (some with >10 mm widths); none of these overlays exhibited reflective cracking that would be expected if the underlying concrete were continuing to expand. Several pairs of notched metal strips were also found installed across selected cracks, presumably to monitor crack growth. In every instance, the notches in the strips were still aligned, indicating no further opening of the cracks. Figure 4 presents typical examples of the concrete overlays and notched metal strips.

Instrumentation for Expansion Monitoring

Despite evidence to suggest that expansion has ceased in the structure, DEMEC targets were installed to re-establish monitoring of the monoliths that were selected for coring in November 2015. Pairs of targets on 500-mm gauge lengths were installed to monitor longitudinal and transverse expansion on each of the four monoliths. Additional pairs of targets on 150-mm gauge lengths were installed at the boundary between monoliths 30 and 29, monoliths 21 and 22, monoliths 20 and 21, and across selected cracks.

Core Extraction

Cores were extracted from monoliths 3, 20, 21, and 30 over two days in November 2015. A total of seventeen 100-mm diameter cores and twenty 50-mm diameter cores were extracted. Logistical constraints limited the number of cores that could be extracted from monoliths 3 and 21, while monolith 20 was so heavily damaged that only one intact core over 200 mm in length could be obtained. The cores were divided between UA and ERDC; UA is focusing on testing for mechanical properties, available alkalis, and residual expansion potential, while ERDC is focusing on petrographic analysis.

Petrography of Cores

Modes of distress were assessed by visual examination of the as-received cores as well as a petrographic analysis performed on polished cross sections conducted according to ASTM C856 [8]. A 25-mm-thick section of a core was cut and prepared for the petrographic analysis. The section for petrographic analysis was polished using diamond-impregnated polishing pads. The polished sample was imaged using a Zeiss Stereo Discovery V12 microscope at magnifications of 5X to 40X. An overall image was obtained for the sample at low magnification, and at least three sites were also selected for higher magnification imaging. Specific attention was given to identifying microcracking, air void structure, aggregate deterioration, and any other possible modes of concrete deterioration that are relevant for service life estimation.

X-ray diffraction (XRD) analysis was performed on the coarse fraction (aggregates) and fines-paste fraction. Once the desired sample was isolated from the concrete, it was crushed and ground until at least 90% of the material passed a #325 sieve (44 μm). The ground specimen was prepared into random powder pack sample holders for XRD measurements. Diffraction patterns to be used for qualitative phase identification were obtained using a Panalytical X'Pert Pro materials research diffractometer equipped with a Co-Kα X-ray source operated at 45kV and 40mA. Diffraction patterns were obtained over a period of 2 hr from 2° to 70° 2θ with a step size of 0.02°. Phase identification was performed using MDI Jade2010 powder diffraction file (PDF) reference databases.

Mechanical Testing of Cores

Selected 100-mm-diameter cores from monoliths 21 (3 cores) and 30 (6 cores) will be tested to determine their mechanical properties. From monolith 30, cores extracted vertically and horizontally will be tested. Testing will include ultrasonic pulse velocity (UPV) per ASTM C597 [9], resonant frequency/dynamic modulus of elasticity per ASTM C215 [10], static modulus of elasticity per ASTM C469 [11], and compressive strength per ASTM C39 [12]. The UPV results may be compared to data reported by Mather from continued investigations of the structure in the early 1950s to determine the relative degradation in mechanical properties over the past sixty-plus years [13]. Following compressive strength testing, the specimens will be preserved in a freezer for available alkali testing.

Available Alkali Testing

Available alkalis will be determined by analyses of expressed pore solution from the mechanical test specimens. ICP-OES will be used to determine Na^+, K^+, Ca^{2+}, and SO_4^{2-}. The hydroxyl concentration of the pore solution will be determined by titration against HCl to a phenolphthalein end point.

Residual Expansion Testing of Cores

50-mm-diameter cores from monoliths 21 (4 cores) and 30 (4 vertical and 4 horizontal cores) will be tested for their residual expansion potential using a modified version of ASTM C1260 recommended by the US Federal Highway Administration [4]. The cores will be instrumented to measure expansion and soaked in a 1N NaOH solution at 38 °C. This test will determine the residual reactivity of the aggregates in the cores by supplying an essentially unlimited quantity of alkalis.

3 RESULTS

3.1 Petrography

Results of petrographic analysis performed on cores from monolith 3 (sample M3-1) and monolith 20 (sample M20-3) are provided herein as these monoliths presented the least and greatest ASR-induced damage from visual observations, respectively. These monoliths were also cored as part of Mather's study.

Optical microscopy

Low-magnification photomicrographs of M3-1 can be seen in Figure 5. Most of the air voids have ASR gel deposits, with reaction rims around the coarse aggregates. Limited aggregate microfracturing is observed primarily in coarse aggregates. However, cracking observed in aggregates did not appear to extend into the mortar fraction of the concrete. Low-magnification photomicrographs of M20-3 can be seen in Figure 6. Most of the air voids have ASR gel deposits, with reaction rims around the coarse aggregates. There are coarse aggregates that have a high degree of internal fracturing. Fracturing in the coarse aggregate particles extends throughout mortar fraction with cracks infilled with ASR gel. A majority of the fine aggregates also exhibit microfracturing and extensive degradation.

X-ray Diffraction (XRD)

XRD measurements were performed to determine mineralogy of various crystalline phases present in the concrete. Figure 7 shows the typical XRD patterns of the coarse fraction and fines/paste fraction of samples M3-1 and M20-3. Phases qualitatively identified to be present are shown at the bottom of Figure 7. The coarse fraction in each sample is primarily composed of quartz with a trace amount of cristobalite. The fines/paste fraction mineral phases identified were quartz, portlandite, ettringite, and alite. The mineralogy of the crystalline components of the coarse aggregate and the fine aggregate portion of the mortar fraction were observed to be nearly identical in both monoliths 3 and 20.

3.2 Additional testing

Tests to determine the mechanical properties, available alkalis, and residual expansion potential of the cores are still in progress. No reportable results are available as of this writing.

4 DISCUSSION

The visual surveys of the lock structure found that, nearly 70 years after Mather's investigation, the severity of concrete cracking varies significantly throughout the structure. Cores examined to date as part of this study were selected from the most-severely damaged sections (monolith 20) and one of the least-severely damaged sections (monolith 3).

Petrographic examination of cores from these monoliths are consistent with the macro-scale observations of cracking during the visual surveys, with significantly more internal micro-cracking, gel deposits, and cracks extending from aggregates into the paste found in sample M20-3 than M3-1.

XRD results indicating the presence of cristobalite and cryptocrystalline quartz in samples from both monoliths are consistent with the use of a single reactive aggregate source in the concrete for the entire structure. This finding supports the hypothesis that the use of different cement types with varying levels of alkali loading contributed to the varying levels of observed ASR-induced damage. Interestingly, the levels of reactive material observed in the aggregates measured during the 2015 petrographic analysis are lower than those reported by Mather. It is possible that the continued reaction following the original petrographic analysis resulted in the observed reduction in reactive material.

Anticipated results from the remainder of the experimental program for this study may contribute to determining if the structure has in fact ceased expanding, and if so, why ASR has ceased (e.g. depletion of alkalis and/or depletion of reactive silica). These results will also determine the relative degradation of the concrete's mechanical properties caused by ASR.

5 CONCLUSIONS AND FUTURE WORKS

A collaboration between The University of Alabama and U.S. Army ERDC has begun with the purpose of re-investigating an historic case of ASR in the Old William Bacon Oliver (Tuscaloosa) Lock. This remains a work in progress, but several conclusions may be drawn from the data presented in this paper:

- There is no discernible difference in the mineralogy of the aggregate used in monoliths 3 and 20, although the degree of distress in these two sections of the structure are very different.
- Therefore, Mather's hypothesis that the two cements used in the construction of the lock were of different alkali contents is likely correct.
- The reduction in the reactive fraction of the aggregate compared to Mather's investigation suggests that ASR continued for some time after his work.
- Expansion of the structure appears to have either ceased or slowed to a negligible rate. It appears unlikely that any substantial expansion has occurred over at least the past 20 to 25 years. However, whether this is a result of alkali depletion, depletion of reactive silica, or both is unclear at this time.

Research activities like those presented herein are in line with the US Army Corps of Engineers' goals to be able to understand and manage its extensive inventory of aging infrastructure. This includes approximately 300 navigation locks, 700 dams, and hundreds of other water resources and flood control infrastructure. Efforts that focus on improving our understanding of AAR-induced damage in existing structures are critical to supporting future management of aging infrastructure assets by the USACE. USACE owns and operates dozens of lock and dam structures that are affected, with various levels of severity, by AAR including both ASR and/or alkali-carbonate reactions. Understanding these deterioration processes, their kinetics, and the future progression of aging is critical to extending the lives of these structures beyond their originally designed service lives.

In many cases, damage to these structures is primarily operational in nature – meaning that the effects of AAR-induced expansion are manifested in issues with operating mechanical systems such as tainter gates, hydraulic operational systems such as valves, and other high tolerance mechanical components. In other cases, stability of structures is a concern due to concrete expansion. In rare cases, expansion is so significant that degradation in mechanical properties (i.e., strength and stiffness) are also a concern. As a result, current research activities in USACE are focused on improving our methods (non-destructive and destructive) to interrogate structures, to perform experiments such as residual expansion to rapidly quantify anticipated additional reactivity, and to be able to fit these results as parameters in long-term simulations that can predict future deleterious operation issues that may result from AAR. Critical to these studies is also understanding the relationships between deterioration metrics and engineering properties. These important deterioration-to-property correlations are seldom made in the field of concrete durability but are essential for asset managers to make risk-informed decisions when prioritizing future operations and maintenance funding to address predicted future deterioration that will occur in a structure.

6 ACKNOWLEDGEMENTS

This study would not have been possible without the assistance of several individuals. Jason Morson and Tyler Johnson from U.S. Army ERDC provided logistical support for site access and operated the coring rigs. Matthew Chandler from The University of Alabama assisted with specimen collection and instrumentation of the lock. Anthony Perkins, Thomas Hood, and Kevin McCauley of the USACE Mobile District helped to arrange permission to instrument and extract cores from the structure.

7 REFERENCES

[1] Mather, B (1952): Cracking of concrete in the Tuscaloosa Lock. Highway Research Board Proceedings (31): 218-233.

[2] McDonald, JE, and Campbell, RL (1977): An investigation of concrete condition, William Bacon Oliver Lock and Spillway, Miscellaneous Paper C-77-5, U.S. Army Engineer Waterways Experiment Station, Vicksburg, MS.

[3] U.S. Army Corps of Engineers, Mobile District (1987): William Bacon Oliver Lock & Dam, Periodic Inspection Report No. 10.

[4] Fournier, B, Berube, MA, Folliard, KJ and Thomas, M (2010): Report on the diagnosis, prognosis, and mitigation of alkali-silica reaction (ASR) in transportation structures. Report No. FHWA-HIF-09-001. Federal Highway Administration, Washington, DC.

[5] Giannini, ER, Folliard, KJ, Zhu, J, Bayrak, O, Kreitman, K, Webb, Z and Hanson, B (2013): Non-Destructive Evaluation of In-Service Concrete Structures Affected by Alkali-Silica Reaction (ASR) or Delayed Ettringite Formation (DEF)—Final Report, Part I. Report No. FHWA/TX-13/0-6491-1. Center for Transportation Research, Austin, TX.

[6] Thomas, MD, Folliard, KJ, Fournier, B, Rivard, P and Drimalas, T (2013): Methods for Evaluating and Treating ASR-Affected Structures: Results of Field Application and Demonstration Projects–Volume I: Summary of Findings and Recommendations. Report No. FHWA-HIF-14-0002. Federal Highway Administration, Washington, DC.

[7] Merz C, Leemann A (2013): Assessment of the residual expansion potential of concrete from structures damaged by AAR. Cement and Concrete Research (52): 182-189.

[8] ASTM C856-14 (2014): Standard Practice for Petrographic Examination of Hardened Concrete. ASTM International, West Conshohocken, PA, United States.

[9] ASTM C597-09 (2009): Standard Test Method for Pulse Velocity through Concrete. ASTM International, West Conshohocken, PA, United States.

[10] ASTM C215-14 (2014): Standard Test Method for Fundamental Transverse, Longitudinal, and Torsional Resonant Frequencies of Concrete Specimens. ASTM International, West Conshohocken, PA, United States.

[11] ASTM C469-14 (2014): Standard Test Method for Static Modulus of Elasticity and Poisson's Ratio of Concrete in Compression. ASTM International, West Conshohocken, PA, United States.

[12] ASTM C39-12 (2012): Standard Test Method for Compressive Strength of Cylindrical Concrete Specimens." ASTM International, West Conshohocken, PA, United States.

[13] Mather, B (1954): Comparative Tests of Soniscopes. Highway Research Board Proceedings 1954 (33): 217-226.

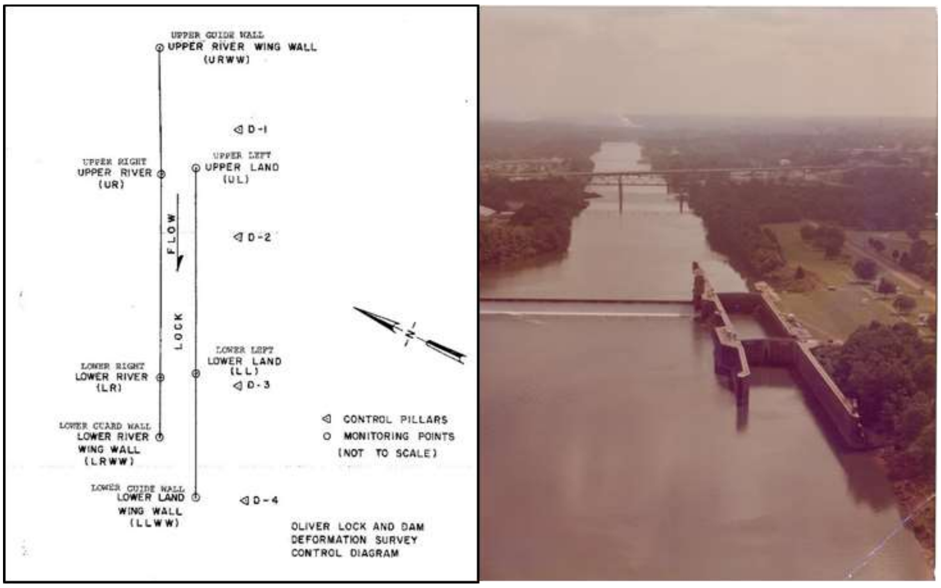

FIGURE 1: Monitoring points and control pillars (left) [3]. View of Black Warrior River and Old Oliver Lock and Dam looking upstream towards Tuscaloosa (right) (photo courtesy USACE Mobile District office).

FIGURE 2: Lock schematic with visual survey damage ratings.

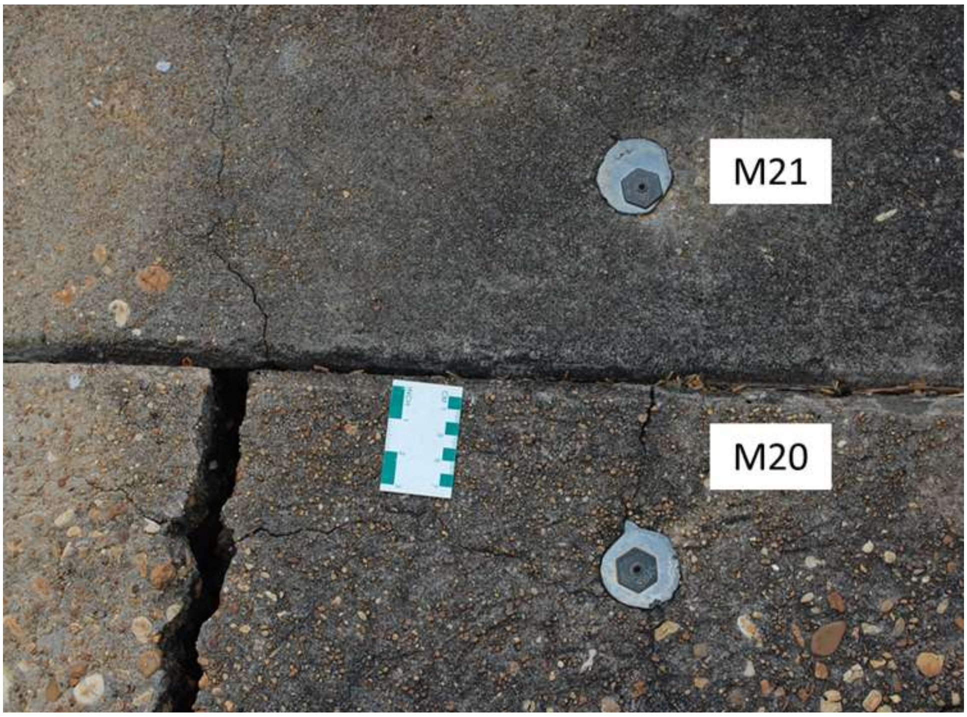

FIGURE 3: Monoliths 20 and 21. Crack openings in monolith 20 exceeded 25 mm in some locations.

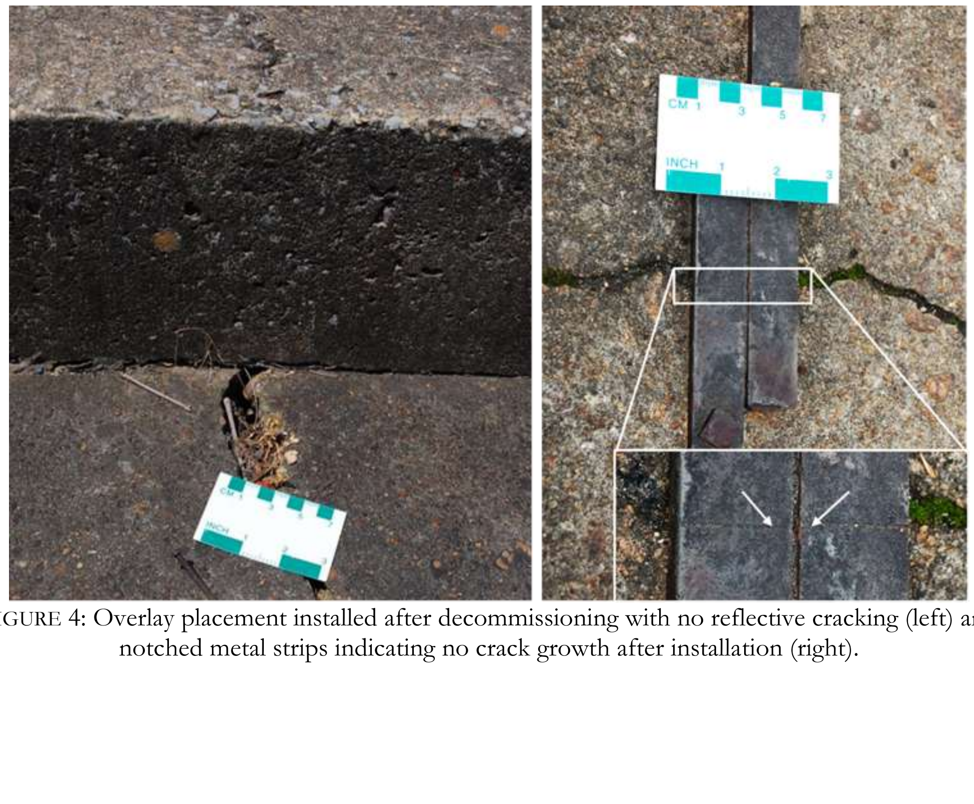

FIGURE 4: Overlay placement installed after decommissioning with no reflective cracking (left) and notched metal strips indicating no crack growth after installation (right).

(a) Low magnification photomicrograph

(b) Low magnification photomicrograph

(c) Low magnification photomicrograph

(d) Low magnification photomicrograph

(e) Low magnification photomicrograph


(f) Low magnification photomicrograph

FIGURE 5: Low-magnification photomicrographs of sample M3-1 from monolith 3.

(a) Low magnification photomicrograph

(b) Low magnification photomicrograph

(c) Low magnification photomicrograph

(d) Low magnification photomicrograph

(e) Low magnification photomicrograph

(f) Low magnification photomicrograph

FIGURE 6: Low-magnification photomicrographs of sample M20-3 from monolith 20.

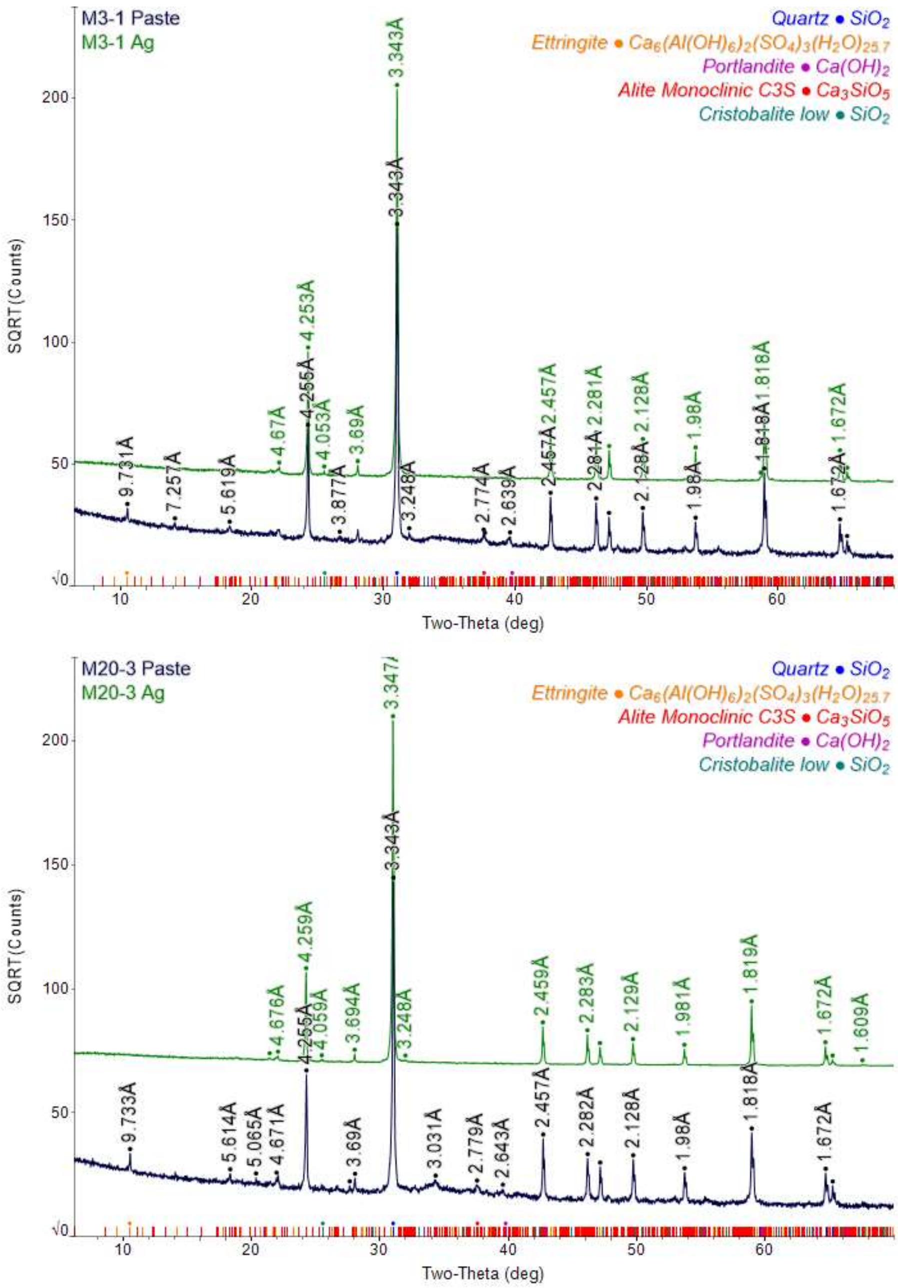

Phase	Aggregate (wt%)		Paste/Fines (wt%)	
	M3-1	M20-3	M3-1	M20-3
Quartz	99.9	99.9	92.5	91.1
Cristobalite (low)	0.1	0.1		
Ettringite			7.2	8.4
Portlandite			0.2	0.2
Alite Monoclinic			0.1	0.3

FIGURE 7: XRD patterns for the coarse fraction and mortar (paste/fines) fraction of samples M3-1 (top) and M20-3 (bottom) with phases qualitatively identified shown at below diffraction patterns.